

1 **Diverging hydrological drought traits over Europe with global warming**

2

3 Carmelo Cammalleri*, Gustavo Naumann, Lorenzo Mentaschi, Bernard Bisselink, Emiliano Gelati,
4 Ad De Roo and Luc Feyen

5

6 European Commission, Joint Research Centre (JRC), 21027 Ispra (VA), Italy.

7 * Correspondence: carmelo.cammalleri@ec.europa.eu; Tel.: +39-0332-78-9869.

8

9 **Abstract**

10 Climate change is anticipated to alter the demand and supply of water at the earth's surface. Since
11 many societal impacts from a lack of water happen under drought conditions, it is important to
12 understand how droughts may develop with climate change. This study shows how hydrological
13 droughts will change across Europe with increasing global warming levels (GWL of 1.5, 2 and 3 K
14 above preindustrial temperature). We employ a low-flow analysis based on river discharge
15 simulations of the LISFLOOD spatially-distributed physically-based hydrological and water use
16 model, which was forced with a large ensemble of regional climate model projections under a high
17 emissions (RCP8.5) and moderate mitigation (RCP4.5) pathway. Different traits of drought,
18 including severity, duration and frequency, were investigated using the threshold level method. The
19 projected changes in these traits identify four main sub-regions in Europe that are characterized by
20 somehow homogeneous and distinct behaviours with a clear southwest/northeast contrast. The
21 Mediterranean and Boreal sub-regions of Europe show strong, but opposite, changes at all three
22 GWLs, with the former area mostly characterized by stronger droughts (with larger differences at 3
23 K) while the latter sees a reduction in all drought traits. In the Atlantic and Continental sub-regions
24 the changes are expected to be less marked and characterized by a larger uncertainty, especially at
25 the 1.5 and 2 K GWLs. Combining the projections in drought hazard with population and
26 agricultural information shows that with 3 K global warming an additional 11 million people and

27 4.5 million ha of agricultural land are projected to be exposed to droughts every year, on average,
28 with the most affected areas located in the Mediterranean and Atlantic regions of Europe.

29

30 **Keywords:** climate change, LISFLOOD, drought, low flow index, Paris agreement, global warming
31 levels.

32 **1. Introduction**

33 As a natural phenomenon, drought occurs in all climates due to a temporary lack of
34 precipitation, which can propagate through the different compartments of the water cycle (Van
35 Loon and Van Lanen, 2012). Drought conditions can be exacerbated by high temperatures, causing
36 an increase in evapotranspiration demand and soil water content draining (e.g., Teuling et al., 2013),
37 and their impacts can be further intensified in areas with an overexploitation of available water
38 resources (Van Loon and Van Lanen, 2013). The strong dependency of drought conditions on the
39 key meteorological forcing suggests likely effects of climate change on future drought severity,
40 duration and frequency, mainly through an alteration of the water balance dynamics (Stagl et al.,
41 2014).

42 Depending on the degree of penetration of the water deficit into the hydrological cycle,
43 drought is commonly classified into meteorological (e.g., precipitation), agricultural (e.g., soil
44 moisture) and hydrological (e.g., river discharge) drought (Wilhite, 2000). Each class of drought
45 may be seen more relevant depending on the specific application, and different effects of climate
46 change are likely to be observed depending on the corresponding analysed indicators (Feng, 2017).
47 In spite of the strong connection between the socioeconomic impacts of droughts and negative soil
48 moisture and river discharge anomalies, fewer studies (e.g., Samaniego et al., 2018; Forzieri et al.,
49 2014) have focused on the climate projection of agricultural and hydrological droughts at European
50 scale compared to meteorological events (e.g., Heinrich and Gobiet, 2012; Spinoni et al., 2018).
51 This focus on meteorological drought mainly relates to the relative simplicity and lower input data
52 requirements of calculating meteorological drought indicators (i.e., Standardised Precipitation
53 Index, SPI) compared to agricultural and hydrological drought indices, with the latter usually
54 requiring simulations from hydrological models. This is also highlighted by the larger emphasis
55 placed on meteorological drought hazard in operational monitoring systems (Barker et al., 2016).
56 Scientific and practical interest in hydrological drought is motivated by the direct and indirect
57 impacts on several socioeconomic sectors, such as energy production, inland water transportation,

58 irrigated agriculture, and public water supply (see the European Drought Impact Inventory,
59 <https://www.geo.uio.no/edc/droughtdb/>). In particular, streamflow drought complements
60 meteorological and soil moisture droughts thanks to its more rapid response to precipitation
61 aberrations compared to groundwater (Tallaksen and van Lanen, 2004).

62 With the raising awareness of climate change, a number of local and regional studies have
63 assessed the potential impacts of climate change on hydrological drought in recent years (e.g.,
64 Brunner et al., 2019; Cervi et al., 2018; Hellwig and Stahl, 2018; Nerantzaki et al., 2019; Rudd et
65 al., 2019; Van Tiel et al., 2018). These studies provide highly detailed insights on the local
66 processes, but their limited spatial extent and lack of homogeneity in the adopted drought
67 indicators, modelling framework and climate scenarios complicate the understanding of large-scale
68 patterns of changes. In spite of the value of continental-scale analyses, few studies have looked at
69 how hydrological droughts could develop across Europe with climate change. They are typically
70 based on pan-European hydrological models forced by climate projections (Feyen and Dankers,
71 2009; Forzieri et al., 2014; Lehner et al., 2006; Marx et al., 2018; Roudier et al., 2016), with ever
72 improved representation of processes in the hydrological models. These improvements include
73 accounting for the effects of water use, more detail in the climate projections (by the use of higher
74 resolution regional climate models), and better accounting for climate uncertainty through multi-
75 model ensembles.

76 Most of past studies portrayed how drought conditions across Europe could look at future
77 points in time (mid- or end- of century) for alternative scenarios of greenhouse gas emissions.
78 However, following the UNFCCC (United Nations Framework Convention on Climate Change)
79 Paris Agreement (UNFCCC, 2015) and the focus on limiting the increase in global average
80 temperature to well below 2 K above the pre-industrial level, the paradigm in climate change
81 studies has shifted from analysing the effects at specific future time windows to evaluating the
82 effect at specific global warming levels (GWLs). To date, there are only few studies that provide
83 insights on how hydrological droughts could change at different GWLs. Roudier et al. (2016) used

84 three hydrological models forced with high resolution regional climate projections to evaluate
85 changes in 10- and 100-year streamflow drought events, with a focus solely on the 2 K scenario.
86 Marx et al. (2018) used three different hydrological models forced by coarse-resolution global
87 climate projections that were downscaled accounting for altitude effects in temperature and
88 precipitation. They used a simple annual 90-th percentile of exceedance of river discharge as index,
89 which is representative of the low flow spectrum. Both studies do not take into account water
90 consumption, which is a key to represent feedbacks between droughts and human activities (Van
91 Loon et al., 2016).

92 To further deepen the understanding on this issue, we evaluate changes in hydrological
93 droughts across Europe between present climate and climate corresponding to different GWLs. We
94 look specifically at 1.5, 2 and 3 K global warming, which represent the different Paris agreement
95 climate change mitigation targets. The study focuses on the threshold level method, allowing for a
96 detailed analysis of different streamflow drought traits, including severity, duration and frequency
97 of the events following an extreme value analysis. These quantities are derived from daily
98 streamflow simulations for the pan-European river network, which are obtained with the
99 LISFLOOD spatially-distributed hydrological model forced with an ensemble of 11 bias-corrected
100 regional climate projections for RCP4.5 and RCP8.5 (Moss et al., 2010). The model incorporate
101 water use modules to reproduce the major sectorial water demands, accounting for the human
102 impact on streamflow propagation, and resulting in a streamflow deficit that represents the
103 integrated deficiency in water availability over the entire upstream catchment.

104 In addition, the effects of the projected changes on two key exposed quantities is evaluated
105 through a drought exposure analysis. It is well-known that droughts affect a large variety of
106 socioeconomic sectors, including agriculture, water supply, energy production and inland water
107 transportation (Meyer et al., 2013), as well as causing losses of ecosystem and biodiversity
108 (Crausbay and Ramirez, 2017). The full quantification of drought risk for all the impacted sectors is
109 a challenging task (Naumann et al., 2015) that goes beyond the scope of this study. Here we focus

110 on the changes between the present and future exposed population and agricultural land, which are
111 key quantities in the major social and economic sectors impacted by drought (e.g., agriculture and
112 livestock farming, and public water supply). The same datasets underlay both the modelling of
113 water usage and the exposure analysis, ensuring consistency in the streamflow drought exposure.

114 **2. Materials and Methods**

115 ***2.1 Climate forcing***

116 In this study, we used projections from 11 combinations of global and regional climate models
117 under two Representative Concentration Pathways (RCP4.5 and RCP8.5) obtained from the EURO-
118 CORDEX initiative (Jacob et al., 2014). The climate projections used in this study were produced
119 by Dosio (2020) by applying a bias-correction quantile mapping approach (Dosio et al., 2012) using
120 the observational dataset EOBSv10 (Haylock et al., 2008). The analysis focuses on 30-year time
121 windows centred on the year when the global models project an increase in global average
122 temperature of 1.5, 2 and 3 K above preindustrial (1881-1910) temperature. For these periods,
123 drought characteristics were contrasted against those derived for the baseline reference period
124 (1981-2010), which has a 0.7 K temperature increase over the preindustrial period.

125 The two RCPs reach the 1.5 and 2 K GWLs around the year 2030 and 2053 (RCP4.5), 2025 and
126 2040 (RCP8.5), on average. The RCP8.5 simulations reach the 3 K GWL at 2063 on average,
127 whereas only one model reaches 3 K warming for RCP4.5. According to the independence of the
128 projected river flow changes from the adopted pathway observed in Mentaschi et al. (2020) for
129 annual minimum (drought), average and maximum (flood) flows, the outputs from both RCPs are
130 merged into a single ensemble. Given that only one model reaches 3 K warming for RCP4.5, the
131 model ensemble is composed by a total of 22 members for the 1.5 and 2 K GWLs and only 12
132 members for the 3 K GWL.

133 ***2.2 Hydrological modelling***

134 Simulations of daily river discharge (Q) were produced at 5×5 km spatial resolution over
135 Europe by forcing the LISFLOOD model (De Roo, 2000) with the bias-corrected climate
136 projections. LISFLOOD is a spatially-distributed physically-based hydrological model that
137 simulates all the main hydrological processes occurring in the land-atmosphere system, including
138 evapotranspiration fluxes (separately for crop transpiration and direct evaporation), infiltration
139 (Xinanjia model), soil water redistribution in the vadose zone (Darcy 1-D vertical flow model),
140 groundwater dynamics (two parallel linear reservoirs), snowmelt (degree-day factor method) and
141 surface runoff (for further details on each module, see Burek et al., 2013). The surface runoff
142 generated in each cell is channelled to the nearest river network cell by means of a routing
143 component based on a 4-point implicit finite-difference solution of the kinematic wave (Chow et al.,
144 1988). The model has been calibrated and validated at global scale on more than 1,200 stations
145 (Hirpa et al., 2018) as part of the EFAS (<https://www.efas.eu/>) and GloFAS
146 (<https://www.globalfloods.eu/>) flood early warning systems.

147 Water abstractions in LISFLOOD consist of five components: (manufacturing) industrial,
148 energy, livestock, domestic and irrigation water demand. While irrigation water demand is
149 modelled dynamically within LISFLOOD, the other four components are downscaled to the model
150 grid cells from country-level data obtained from EUROSTAT and AQUASTAT. High resolution
151 data from the Land-Use based Integrated Sustainability Assessment (LUISA) Territorial Modelling
152 Platform (Jacobs-Crisioni et al., 2017) were used for the spatial downscaling of the socioeconomic
153 drivers of present and future water use, with projected data consistent with the EU economic,
154 budgetary, and demographic projections (EC, 2015). These data are produced as part of the
155 “production and visualization of territorial indicators” component of the LUISA platform and
156 distributed through the Territorial Dashboard (<http://urban.jrc.ec.europa.eu/t-board>). Maps cover the
157 EU Member States and several Western Balkan countries until 2050 at a detailed spatial resolution
158 ($\sim 100\text{m}^2$) (Jacobs-Crisioni et al., 2017). Since the LUISA population and land use projections
159 cover up to 2050, these quantities were assumed static thereafter.

160 In detail, irrigation is estimated dynamically at the model time step (daily in this study) based
161 on two distinct methods for crop irrigation and paddy-rice irrigation, as defined from land use maps.
162 In the former, the demanded water amount by the crop (transpiration) is compared to the available
163 water in the soil and the irrigation is modelled to keep the soil water content at field capacity (also
164 accounting for the different efficiency of the irrigation systems). In the paddy-rice irrigation instead,
165 a defined water-level is maintained during the whole irrigation season (also accounting for soil
166 percolation). Maximum crop transpiration is function of potential evapotranspiration through a
167 crop-specific efficiency coefficient.

168 Downscaling of the livestock water demand at grid scale was performed as described in
169 Mubareka et al. (2013), by computing the water demand of each livestock category (e.g., cattle,
170 pigs, sheep) separately. Public water withdrawal was downscaled using a land use proxy approach
171 (Vandecasteele et al., 2014), assuming that public water withdrawal is the total water withdrawn in
172 urban areas (i.e., commercial/service are negligible). Similarly, industrial water demand was
173 disaggregated using the corresponding land use classes in the LUISA platform (Bisselink et al.,
174 2018), and projections of the Gross Value Added of the industrial sector were used to simulate
175 future demand. Water demand for energy and cooling is computed with a relatively similar
176 approach, with national data downscaled to the locations of large power thermal power stations
177 registered in the European Pollutant Release and Transfer Register data base (E-PRTR). Future
178 changes in energy water use are simulated according to the electricity consumption projections from
179 the POLES model (Prospective Outlook on Long-term Energy Systems, Keramidas et al., 2017).

180 **2.3 Drought modelling**

181 The hydrological drought modelling approach used in this study is analogous to the
182 methodology used to estimate the low-flow indicator used in the European Drought Observatory
183 (EDO) (Cammalleri et al., 2017). The key quantity is the water deficit computed from an unbroken
184 sequence of discharge (Q) values below a defined low-flow threshold. We used the 85-th percentile,
185 Q_{85} , derived for the present climate as a threshold both in the present and future scenarios, with the

186 aim to estimate how droughts under present climate conditions will be projected under climate
187 change.

188 According to the theory of runs (Yevjevich, 1967), a continuous period with river flow values
189 below the defined low-flow threshold is considered as a drought event, of which the severity is
190 quantified by the total deficit (D , represented by the area enclosed by the threshold and the
191 streamflow time series). Other key traits of drought are the duration, quantified by the length of the
192 drought in days (N), and the temporal frequency of the events, which can be expressed as return
193 period (T).

194 In order to avoid potential bias in the analysis with the inclusion of minor events and to ensure
195 the independence among events, two post-processing corrections were applied after selection of the
196 events below the threshold: 1) consecutive events with an inter-event time smaller than 10 days
197 were pooled together (Zelenhasić and Salvai, 1987), and 2) small isolated events (of duration less
198 than 5 days) were removed from the analysis (Jakubowski and Radczuk, 2004). Specifically, the
199 first correction accounts for the potential statistical inter-dependency of events that are close in
200 time, whereas the second reduces the effects of the uncertainty in the defined threshold by removing
201 the events with discharge values very close to the threshold only for a short period of time.

202 Following this definition, a sequence of drought events for both the baseline period and the
203 three GWLs were derived. Given the huge variability of D values across the European domain due
204 to differences in hydrological regimes and size of river basins, the changes in drought severity are
205 expressed as relative differences (%) from the values in the baseline period (1981-2010). The series
206 of D events was fitted according to the Pareto Type II distribution (also known as Lomax
207 distribution, a special case of the Generalized Pareto Distribution with location parameter equal to
208 zero), formally expressed as:

$$209 \quad F(D; \alpha; \lambda) = 1 - \left(1 + \frac{D}{\lambda}\right)^{-\alpha} \quad (1)$$

210 where α and λ are the strictly positive shape and scale parameters, respectively, derived from the
211 sample according to the maximum likelihood method. The fitted distributions allow computing the
212 return period associated to a specific D value (T , the average occurrence interval which refers to the
213 expected value of the number of realizations to be awaited before observing an event whose
214 magnitude exceeds D ; Serinaldi, 2015), or to be used in reverse to estimate the D value associated
215 to a specific return period. More details on the implementation of the drought indicator over Europe
216 can be found in Cammalleri et al. (2017), including a validation against some major past drought
217 events. An analogous validation at global scale can be found in Cammalleri et al. (2020), where a
218 goodness-of-fit test for the Lomax distribution is also performed.

219 **2.4 Population and agricultural land exposed to streamflow drought**

220 In order to quantify how global warming could change exposure to streamflow drought in
221 Europe, different exposed quantities can be analysed depending on the impacted sector. Agriculture
222 and livestock farming, and public water supply seem to be the two most reported economic sectors
223 according to the European Drought Impact Inventory (EDII,
224 <https://www.geo.uio.no/edc/droughtdb/>). As a result, we focus the exposure analysis on population
225 and agricultural land. For the baseline we used the map of agricultural areas from the CORINE land
226 Cover (EEA, 2016) and the population density from the LUISA Territorial Modelling Platform
227 (Batista e Silva et al., 2013). Consistently with the hydrological simulations, for future time slices
228 the land use and population projections of LUISA were used up to 2050.

229 The spatial data of population and agricultural land were summed over NUTS 2 statistical
230 regions (or equivalent for EU-neighbour countries according to Eurostat,
231 <https://ec.europa.eu/eurostat/web/nuts/statistical-regions-outside-eu>). Then, the expected year-
232 average exposed population and agricultural land were computed by equally dividing over time the
233 changes in drought exposure caused by the median (over the NUTS 2) changes in drought
234 frequency of an event with a 10-year return period in the baseline. Following this approach, the
235 exposure associated to a present 10-year or more intense drought is simply averaged over the

236 period, obtaining a standardized year-average quantity. Finally, changes over NUTS 2 regions were
237 further aggregate to country scale.

238 **3. Results**

239 *3.1 Evaluation of the changes in main drought traits*

240 *3.1.1 Drought severity*

241 Figure 1 shows the ensemble-median relative change in severity of a 10-year drought between
242 the baseline and the GWLs, with positive (negative) values indicating a higher (lower) drought
243 severity with warming compared to the reference. The projected changes are considered robust
244 when at least 2/3 of the ensemble members agree on the sign of change (no-agreement otherwise),
245 which is a simplification of the approach proposed by Tebaldi et al. (2011) and applied over Europe
246 by Dosio and Fischer (2018).

247 The spatial maps depicted in Figure 1 highlight a strong divergence in the projected changes of
248 drought severity with warming over Europe, with four macro-regions (delimited in Figure 1 lower-
249 right panel) displaying somewhat homogeneous behaviour. The four macro-regions were derived by
250 computing for each country the predominant change for the three GWLs, then by combining the
251 countries with similar features. A similar rough subdivision, which is in line with the IPCC AR5
252 European macro regions (Kovats et al., 2014) derived from a principal component analysis of 20
253 environmental-relevant variables performed by Metzger et al. (2005), has been already used in
254 previous early studies at continental-scale (i.e., Feyen and Dankers, 2009; Lehner et al., 2006), and
255 for this reason it will be adopted in all the subsequent analyses.

256 In the Mediterranean sub-region (i.e., Iberian Peninsula, Italy, Greece and the Balkans)
257 generally more severe droughts are projected, whereas in the Boreal sub-area (i.e., Scandinavia
258 peninsula and Baltic countries) drought severity is expected to reduce almost everywhere. The
259 projected changes are less marked in two transition regions, but, in general, they point towards more
260 severe droughts in the Atlantic (i.e., British Isles, France, Belgium and the Netherlands) and less

261 severe droughts over the Continental sub-area (Germany, Poland and eastern European countries).
262 Overall, these patterns of change become stronger and more robust with increasing warming.

263 The strongest increase in drought severity is projected for Portugal, Spain and Greece, where
264 the fraction of rivers with an increase in deficit of more than 50% at 3 K is 99, 80 and 75%,
265 respectively. If climate stabilizes at 2 K, streamflow drought severity is lower than at 3 K, but still
266 at least 50% higher than in the baseline for half of the rivers of Portugal and Spain, and 35% of
267 Greece. Capping global warming at 1.5 K would further limit the increase in severity, with only 21,
268 20 and 14% of the rivers of Portugal, Spain and Greece expected to experience an increase in
269 drought severity of more than 50%.

270 Over the Atlantic region (apart from Iceland), streamflow droughts are generally projected to
271 also become more severe with global warming. The south of France shows a pattern towards more
272 severe flow deficits with warming that is similar to that projected for most of the Mediterranean.
273 For the other parts of the Atlantic sub-region the changes are less pronounced. Keeping warming to
274 2 K or below would limit the increase in severity for most of the region to below 25% compared to
275 the baseline. At 3 K warming, the increase in severity could reach up to 50%. In some parts of the
276 Atlantic sub-region, such as the Seine river catchment in France (northern France), at lower levels
277 of warming the climate models do not agree on the sign of the change, or show a small trend
278 towards less severe droughts. Yet, with stronger warming the signal of change reverses towards
279 more severe droughts.

280 Over most of the Continental sub-region there is a trend towards less severe droughts with
281 global warming. On the one hand, this trend is somewhat more pronounced in upstream Danube
282 tributaries that drain the Alps to the east. In many downstream Danube tributaries in Hungary,
283 Romania and Bulgaria, on the other hand, streamflow droughts are projected to become more severe
284 (in agreement with the results reported in Stagl and Hattermann, 2015). At low levels of global
285 warming (1.5 and 2 K) most of Germany is expected to experience less severe droughts. At high

286 levels of warming (3 K), however, western parts of Germany are projected to experience and
287 inverse trend while the rest shows a large uncertainty in the projected changes. In contrast to most
288 of the Continental sub-area, projections of streamflow drought severity show an increase with
289 global warming over Denmark.

290 Finally, in most of the Boreal region, streamflow drought deficits is expected to become
291 progressively less severe with warming. At 3 K warming streamflow droughts could be half as
292 severe compared to the baseline, with few notable exceptions in southern Sweden.

293 ***3.1.2 Drought duration***

294 Figure 2 shows the fraction of each sub-region (presented in the lower-right panel of Figure 1)
295 for which a certain degree of change in drought duration is projected for the different warming
296 levels. There is a clear upward climate change-induced trend in the fraction of the Mediterranean
297 sub-region that will be exposed to longer droughts. When keeping global warming limited to 1.5 K,
298 droughts are projected to last more than 5-days longer in about 40% of the Mediterranean, with a
299 prolongation above 15 days in slightly more than 5% of the area. At 3 K warming, however,
300 streamflow droughts will last longer in 80% of the area and nearly half of the sub-region could face
301 an increase in drought duration of at least 10 days.

302 An upward, but less pronounced, trend in drought duration with global warming is also
303 projected for most of the Atlantic sub-region. At 1.5 K GWL, the area with a decrease in drought
304 duration (about 30%) is comparable to the area with an increase, with no clear signal in about 40%
305 of the domain. With higher levels of warming, the area with a shorter drought duration shrinks,
306 while the fraction of land that is expected to face longer droughts steadily expands. At 3 K GWL,
307 droughts are projected to last longer in about 75% of the sub-region, hence similar to what can be
308 observed for the Mediterranean. Yet, for only 10% of the area, drought duration is expected to
309 increase by more than 10 days.

310 In the Continental sub-region, the area that shows a decrease in drought duration is around 65%
311 at 1.5 K, which slightly reduces in extent with increasing warming. Yet, over this area droughts are
312 expected to progressively shorten with further warming. At 3 K warming, with droughts lasting at
313 least 10 and 15 days shorter over more than 30 and 10% of the region, respectively. Drought
314 duration is projected to increase over a small part (20% at 3 K) of the domain, mainly
315 corresponding to Bulgaria.

316 Over the Boreal sub-region, droughts are projected to become shorter with global warming over
317 practically the whole domain. At 1.5 K warming, drought duration is expected to be at least 15 days
318 shorter in 20% of the area, which grows to 50% of the area at 3 K warming. For all sub-regions, the
319 fraction of area with no-agreement in future drought duration tends to reduce with increasing global
320 warming, and this signal is very consistent among all the climate projections. At 3 K warming,
321 projections show that less than 15% of the domain under study have no agreement in the direction
322 of change in drought duration.

323 ***3.1.3 Drought frequency***

324 Figure 3 shows the frequency distribution of drought return periods for the three GWLs
325 corresponding to an event with a return period (T) of 10 years under baseline climate. In these plots,
326 values greater than 10 can be interpreted as a reduction in drought frequency (an event with $T = 10$
327 years in the baseline will become rarer), whereas values lower than 10 represent an increase in
328 drought frequency (an event with $T = 10$ years in the baseline will become more common).

329 The frequency distributions of T values for the Mediterranean (upper-left panel) show a clear
330 shift towards more recurrent droughts. At 1.5 K warming the peak value is around 8 years, which
331 further reduces to 7 and 6 years at 2 and 3 K warming, respectively. At 3 K warming the lower tail
332 of the distribution falls below 4 years. In nearly 10% of the rivers, drought deficits that in baseline
333 climate happen once in 10 years are expected to occur at least 2.5 times more frequent with 3 K
334 warming. In the Atlantic sub-region the central value also reduces with warming, yet the overall

335 reduction is less pronounced than in the Mediterranean sub-area, with a median value around 7
336 years at 3 K warming. In the Continental region, droughts will in general become less frequent with
337 a central value between 12 and 13 years at all warming levels, even if the fraction of river cells with
338 an increase in frequency (around 28% at 3 K) is larger than that with an increase in drought duration
339 (less than 20% at 3 K, see Figure 2). In the Boreal sub-area the shift towards less frequent droughts
340 is much more pronounced, with projected return periods concentrated around 20, 30 and 40 years
341 for 1.5, 2 and 3 K warming, respectively.

342 In addition to the shifts in central value of the frequency distributions, it is possible to observe
343 an increase with warming in the spread around the central value for all regions. Additionally,
344 changes opposite to the general trend can be observed in all regions. For example, over very few
345 locations in the Mediterranean sub-region, such as some Alpine mountain drainage basins in
346 northern Italy, drought conditions could become less severe and frequent (see also drought severity
347 changes in Figure 1). In the Atlantic region, the small secondary peak of T values > 20 years
348 corresponds to areas where droughts are projected to occur less frequently with global warming,
349 such as Iceland and few tributaries from the Rhône that originate in the Alps (similarly to what was
350 observed on drought severity in Figure 1). Even in the Boreal region a small fraction of the sub-
351 domain shows an increase in drought frequency, while drought duration is projected to reduce
352 practically everywhere. This is confirmed by the slight reduction in the frequency median value at 3
353 K GWL (26 years, compared to 27 years at 2 K).

354 The results reported in Figure 3 for the 10-year return period can be seen as representative of
355 the behaviour at other return periods as well. To support this consideration, the data in Figure 4
356 report the sub-region median relative changes at the three GWLs for events with a baseline return
357 period of 3, 5, 10, 20 and 50 years. The plots clearly show how all the return periods have similar
358 dynamics, with the only notable exception represented by the more marked reduction in median
359 relative change of high return periods for the 3 K GWL in the Boreal sub-region (i.e., 20 and 50

360 years). It is also worth to point out how even if the dynamics are comparable among the different
361 return periods, the magnitude of the relative changes is higher for the longer return periods.

362 ***3.2 Population and agricultural land exposed to drought***

363 Figure 5 shows the changes with respect to the baseline in population projected to be exposed to
364 streamflow drought at country scale (percentage relative changes are also reported as numbers next
365 to the bars). Total changes for the four macro-regions and the entire domain (TOT) are summarised
366 in Table 1. Aggregated over the whole domain, about 1.5 million fewer people are expected to be
367 annually exposed to drought at 1.5 K GWL compared to the baseline period, which reverses to an
368 increase of about 2.5 and 11 million people/year compared to baseline human exposure at 2 and 3 K
369 GWLs, respectively. This is because at 1.5 K the increase in population exposed annually in the
370 Mediterranean (2.4 million) and Atlantic (less than 0.1 million) sub-regions is outweighed by the
371 reduction in exposure in the Boreal (-0.6 million) and, most importantly, Continental (-3.4 million)
372 sub-regions. Projections in the Mediterranean and Atlantic sub-regions show a progressive increase
373 in population exposed (up to a total of 15.8 million people/year for 3 K GWL over the two regions),
374 while in the Boreal and Continental combined human exposure to droughts is expected to remain
375 roughly the same for all three GWLs (i.e., -3.9, -5.4 and -4.7 million/year at 1.5, 2 and 3 K,
376 respectively).

377 Spain is projected to have the largest absolute increase in population exposed to drought with
378 global warming, with an almost doubling (+3.8 million/year) of the number of people exposed to
379 drought each year at 3 K GWL. In relative terms, the relative increase in population exposure at 3K
380 is also high in Portugal (+81%), United Kingdom (+58%) and France (+52%). The largest absolute
381 decrease in population exposed is expected for Germany at 1.5 and 2 K GWL (-1.8 and -1.7 million
382 people/year) and Poland at 3 K GWL. The transition of several areas in Germany from a decrease in
383 drought to uncertain conditions (see as an example western Germany in Figure 1) explains the
384 lower number of exposed people at 3 K (-0.9 million people/year) compared to Poland (-1.2 million

385 people/year). The strongest reduction in population exposure in relative terms is expected for
386 Norway, Iceland and Lithuania (up to 65, 87 and 85%, respectively).

387 Exposure of agricultural land (Figure 6 and Table 2) shows similar trends as for population.
388 Aggregated over Europe, the change in exposure is projected to be balanced in the exposed
389 agricultural land at 1.5 K GWL (net increase of 0.1 million ha/year), whereas at higher warming
390 levels exposure of agricultural land increases to 1.2 and 4.5 million ha/year at 2 and 3 K,
391 respectively. This can be explained by the expected steady increase in agricultural land exposed to
392 drought in the Mediterranean and Atlantic sub-regions (up to 6 million ha/year combined at 3 K),
393 which is not counterbalanced at the highest warming by the agricultural land being less exposed to
394 drought in the Boreal and the Continental sub-regions (-1.3 million ha/year at 1.5 K and -1.5 million
395 ha/year at 3 K). In absolute numbers, Spain shows the largest projected increase in the agricultural
396 land exposed at all GWLs, with an additional 0.9 million ha/year at 1.5 K to 2.6 million ha/year at 3
397 K (corresponding to a relative increase of about 35 and 97%, respectively). Relative changes are
398 expected to be quite notable for other Mediterranean countries as well, such as Portugal and Greece,
399 reaching almost 120 and 77% at 3 K, respectively.

400 **4. Discussion**

401 The projections of severity, duration and frequency underline some common features in future
402 streamflow drought in Europe. The uncertainty in the projections is more marked at the 1.5 and 2 K
403 GWLs, whereas patterns are more statistically robust at higher warming, as also observed by Marx
404 et al. (2018) for minimum flows. The magnitude of the projected changes increases in general with
405 warming for all the drought traits, with only limited areas interested by an inversion in the trend.
406 The main pattern is a strengthening of the dichotomy between southern but also western parts of
407 Europe that will become more prone to droughts and a wetting north, which is a trend that is already
408 ongoing according to Stagge et al. (2017). This result is also in line with other studies that projected
409 streamflow droughts focusing on specific temporal horizons (Lehner et al., 2006; Feyen and

410 Dankers, 2009; Stahl et al., 2012; Forzieri et al., 2014) or on agricultural (e.g., Samaniego et al.,
411 2018) and meteorological (e.g., Gudmundsson and Seneviratne, 2016; Spinoni et al., 2018)
412 droughts. Hence, there is growing consensus in the community on the main patterns of climate-
413 induced changes on drought conditions in Europe.

414 Overall, the Mediterranean sub-region shows the strongest negative change, with droughts
415 projected to become more severe, last longer and happen more frequently already at 1.5 K GWL.
416 The combined effects of increasing temperature and decreasing summer precipitation (Dubrovský et
417 al., 2014; Vautard et al., 2014) are expected to result in a further exacerbation of water deficits in an
418 area already prone to limited water resources. This agrees with global studies that identify the
419 Mediterranean as a hot spot for climate change, even if the targets set by the Paris agreement will be
420 met (Gu et al., 2020), and also with the study of Guerreiro et al. (2017) on the potential occurrence
421 of multi-year droughts in major Iberian water resource regions.

422 Symmetrically, the Boreal sub-region is projected to experience a general reduction in all
423 drought traits, as the increase in precipitation will likely outweigh the increase in evaporative
424 demand due to elevated temperatures (Jacob et al., 2018). Over this region, similarly to the Alps
425 (Donnelly et al., 2017), increasing winter precipitation and higher temperatures is expected to result
426 in higher winter flows, when river flows are typically at their lowest (Gobiet et al., 2014).

427 In the other two sub-regions the projections are less uniform, with more variation in the signal
428 and robustness of the projections with global warming. In the Atlantic sub-region the increase in
429 droughts at 3 K is expected to be less pronounced compared to the Mediterranean, but similarly
430 robust, while at lower warming levels there is large uncertainty in the projections. In some river
431 basins, such as the Seine in northern France, a positive (i.e., less droughts) or uncertain trend is
432 projected for low levels of global warming, while at higher levels of warming drought conditions
433 are projected to worsen. This is related to the fact that at higher levels of warming the atmospheric
434 demand (evapotranspiration) rises faster than supply due to the combination of a strong rise in

435 temperature and a slight or uncertain increase in annual precipitation and a decline in summer
436 precipitation (Kotlarski et al., 2014).

437 In the Continental sub-region the projected overall decrease in droughts is rather
438 inhomogeneous in strength. In upstream Danube tributaries draining the Alps there is a strong trend
439 towards less severe droughts as winter flows increase due to changes in snow accumulation and
440 melt caused by increased winter precipitation and higher temperatures (Forzieri et al., 2014; Marx et
441 al., 2018). In downstream reaches of the Danube, more severe droughts are projected due to a
442 reduction in summer flows caused by an increased evaporative demand and less precipitation. Also
443 in Germany, the trend towards less severe droughts for the Paris warming targets is reversed at
444 higher warming as the increasing natural and human demand in drier summers outbalance higher
445 annual supply. This is the case especially in western parts of Germany such as downstream reaches
446 of the Rhine (Bosshard and Kotlarski, 2014).

447 This shows that the projected trends relate to the interplay between supply (precipitation),
448 atmospheric demand (evapotranspiration) and human water use. Dosio and Fischer (2018) showed
449 that precipitation will increase over most continental and northern parts of Europe (by +10-25% at 3
450 K), but to a lesser extent in summer months (changes with 3 K between -5% at middle latitudes of
451 Continental Europe to +10-15% at higher latitudes in the Boreal region), when natural and human
452 demand are highest. As a result, short duration droughts could happen more frequently in some
453 catchments even when summer supply does not change drastically due to the growth in natural
454 (because of rising temperatures) and human demand. In the case of longer drought events, the
455 imbalances between supply and demand over summer may be mitigated by the increase in
456 subsurface storages at the start of the summer season due to elevated precipitation amounts during
457 the other seasons, but also potentially exacerbated in case of multi-annual summer droughts. In
458 high-regulated basins in Europe, accounting for water uses and its temporal evolution is key to
459 accurately represent streamflow drought in the anthropocene, when both natural and human induced
460 factors influence drought propagation even further (Van Loon et al., 2016).

461 **5. Summary and Conclusions**

462 This study analysed how the main characteristics of hydrological droughts are expected to
463 change over Europe due to global warming. Projections in drought severity, duration and frequency
464 based on river water deficits highlight some common features and spatial patterns in future drought
465 conditions across Europe. The Mediterranean sub-region, which already suffers most from water
466 scarcity, is projected to experience the strongest negative effects of climate change on drought
467 conditions. With increasing global warming, streamflow deficits in this region expected to happen
468 more frequently, become more severe and last longer. Symmetrically, the Boreal sub-area is
469 projected to face a consistent decrease in drought severity, duration and frequency.

470 In the Atlantic and Continental sub-regions the projections are less uniform, although over most
471 of the Atlantic drought conditions are projected to worsen, while they generally will become less
472 intense over Continental Europe. Despite the use of a large ensemble of climate models, there is still
473 a substantial uncertainty in the projections in these regions, even if changes at 3 K are mostly well
474 defined. The uncertainty is bigger for the 1.5 and 2 K GWLs, which suggests that there is still large
475 disagreement among the models in possible changes in drought conditions in these areas when
476 warming could be stabilised at the targets set in the Paris climate agreement.

477 The general patterns observed in this study are in line with other studies focused on specific
478 temporal horizons rather than warming levels (Forzieri et al., 2014; Spinoni et al., 2018; Stahl et al.,
479 2012), as well as with the results of Marx et al. (2018) on the simple daily streamflow percentile. In
480 addition to that, this study provides a comprehensive analysis of different traits of streamflow
481 droughts (i.e., severity, duration and frequency), it accounts for of the effects of human activities
482 through the modelling of water demand, and it focuses on policy-relevant GWLs. The findings
483 provide information that can be used as a basis to evaluate the implications at European scale of
484 climate mitigation policies.

485 In this regard, it is clear that with higher warming the changes in drought traits are expected to
486 be more marked, even if the spatial patterns of the areas with increasing/decreasing drought
487 conditions are rather similar for the three GWLs here analysed. The exposure analysis with
488 population density and agricultural land highlights how at lower warming levels positive and
489 negative changes in exposure are expected to be balanced across Europe. However, at higher GWLs
490 the increase in population and agricultural exposure in southern and western parts of Europe is
491 projected to outweigh the effects of less severe droughts in the less populated north and most of
492 continental and eastern Europe. At 3 K warming this could result in an additional 11 million people
493 and 4.5 million ha exposed each year to drought conditions that currently are expected to happen
494 once every 10 years or less. The projected changes in exposure to drought will pose considerable
495 challenges for agriculture and water provision in densely populated and economically pivotal areas,
496 especially in southern Europe.

497

498 **Data availability.** All data are available via the EDO web portal (<https://edo.jrc.ec.europa.eu/>) upon
499 request. A selected subset of the outputs will be made available through the JRC-DRMKC Risk
500 Data Hub (<https://drmkc.jrc.ec.europa.eu/risk-data-hub>).

501 **References**

- 502 Barker, L.J., Hannaford, J., Chiverton, A., Svensson, C., 2016. From meteorological to hydrological
503 drought using standardised indicators. *Hydrol. Earth Syst. Sci.* 20, 2483-2505.
504 doi:10.5194/hess-20-2483-2016.
- 505 Batista e Silva, F., Gallego, J., Lavalle, C., 2013. A high-resolution population grid map for Europe.
506 *J. Maps* 9(1), 16-28. doi: 10.1080/17445647.2013.764830.
- 507 Bisselink, B., Bernhard, J., Gelati, E., Adamovic, M., Guenther, S., Mentaschi, L., De Roo, A.,
508 2018. Impact of a changing climate, land use, and water usage on Europe's water resources.
509 JRC Technical Reports, EUR 29130 EN, Publications Office of the European Union,
510 Luxembourg, 86 pp. doi:10.2760/847068.
- 511 Bosshard, T., Kotlarski, S., 2014. Hydrological climate-impact projections for the Rhine river:
512 GCM-RCM uncertainty and separate temperature and precipitation effects. *Hydrometeor.*
513 15, 697-713. doi:10.1175/JHM-D-12-098.1.
- 514 Brunner, M.I., Liechti, K., Zappa, M., 2019. Extremeness of recent drought events in Switzerland:
515 Dependence on variable and return period choice. *Nat. Hazards Earth Syst. Sci.* 19(10),
516 2311-2323. doi:10.5194/nhess-19-2311-2019.
- 517 Burek, P., van der Knijff, J.M., De Roo, A., 2013. LISFLOOD: Distributed Water Balance and
518 Flood Simulation Model. JRC Technical Reports, EUR 26162 EN, Publications Office of
519 the European Union, Luxembourg, 142 pp. doi:10.2788/24719.
- 520 Cammalleri, C., Vogt, J., Salamon, P., 2017. Development of an operational low-flow index for
521 hydrological drought monitoring over Europe. *Hydrol. Sci. J.* 62(3), 346-358.
522 doi:10.1080/02626667.2016.1240869.

523 Cammalleri, C., Barbosa, P., Vogt, J.V., 2020. Evaluating simulated daily discharge for operational
524 hydrological drought monitoring in the Global Drought Observatory (GDO), *Hydrol. Sci. J.*
525 65(8), 1316-1325. doi:10.1080/02626667.2020.1747623.

526 Cervi, F., Petronici, F., Castellarin, A., Marcaccio, M., Bertolini, A., Borgatti, L., 2018. Climate-
527 change potential effects on the hydrological regime of freshwater springs in the Italian
528 northern Apennines. *Sci. Total Environ.* 622-623, 337-348.
529 doi:10.1016/j.scitotenv.2017.11.231.

530 Chow, V.T., Maidment, D., Mays, L.W., 1988. *Applied Hydrology*. New York, McGraw-Hill.

531 Crausbay, S.D., Ramirez, A.R., 2017. Defining ecological drought for the twenty-first century. *Bull.*
532 *Am. Meteorol. Soc.* 2543-2550. doi:10.1175/BAMS-D-16-0292.1.

533 De Roo, A., Wesseling, C., Van Deursen, W., 2000. Physically based river basin modelling within
534 a GIS: the LISFLOOD model. *Hydrol. Process.* 14, 1981-1992. doi:10.1002/1099-1085.

535 Donnelly, C., Greuell, W., Andersson, J., Gerten, D., Pisacane, G., Roudier, P., Ludwig, F., 2017.
536 Impacts of climate change on European hydrology at 1.5, 2 and 3 degrees mean global
537 warming above preindustrial level. *Climatic Change* 143, 13-26. doi:10.1007/s10584-017-
538 1971-7.

539 Dosio, A., 2020. Mean and extreme climate in Europe under 1.5, 2, and 3°C global warming. EUR
540 30194 EN, Publications Office of the European Union, Luxembourg, 2020, ISBN 978-92-
541 76-18430-0, doi:10.2760/826427, JRC120574.

542 Dosio, A., Fischer, E.M., 2018. Will half a degree make a difference? Robust projections of indices
543 of mean and extreme climate in Europe under 1.5°C, 2°C, and 3°C global warming. *Geoph.*
544 *Res. Letters* 45(2), 935-944. doi:10.1002/2017GL076222.

545 Dosio, A., Paruolo, P., Rojas, R., 2012. Bias correction of the ENSEMBLES high resolution
546 climate change projections for use by impact models: Analysis of the climate change signal.
547 J. Geoph. Res. Atm. 117(17). doi:10.1029/2012JD017968.

548 Dubrovský, M., Hayes, M., Duce, P., Trnka, M., Svoboda, M., Zara, P., 2014. Multi-GCM
549 projections of future drought and climate variability indicators for the Mediterranean region.
550 Reg. Environ. Change 14, 1907-1919. doi:10.1007/s10113-013-0562-z.

551 EC, 2015. The 2015 Ageing Report - Economic and budgetary projections for the 28 EU Member
552 States (2013-2060). European Commission. doi:10.2765/877631.

553 EEA, 2016. Corine Land Cover (CLC), Version 18.5.1. Release Date: 19-09-2016. European
554 Environment Agency. <https://land.copernicus.eu/pan-european/corine-land-cover>.

555 Feng, S., 2017. Why do different drought indices show distinct future drought risk outcomes in the
556 U.S. Great Plains? J. Climate 30, 265-278. doi: 10.1175/JCLI-D-15-0590.1.

557 Feyen, L., Dankers, R., 2009. Impact of global warming on streamflow drought in Europe. J.
558 Geophys. Res. 114, D17116. doi:10.1029/2008JD011438.

559 Forzieri, G., Feyen, L., Rojas, R., Flörke, M., Wimmer, F., Bianchi, A., 2014. Ensemble projections
560 of future streamflow droughts in Europe. Hydrol. Earth Syst. Sci. 18(1), 85-108.
561 doi:10.5194/hess-18-85-2014.

562 Gobiet, A., Kotlarski, S., Beniston, M., Heinrich, G., Rajczak, J., Stoffel, M., 2014. 21st century
563 climate change in the European Alps - A review. Sci. Tot. Environ. 493, 1138-1151.
564 doi:10.1016/j.scitotenv.2013.07.050.

565 Gu, L., Chen, J., Yin, J., Sullivan, S.C., Wang, H.-M., Guo, S., Zhang, L., Kim, J.-S., 2020.
566 Projected increases in magnitude and socioeconomic exposure of global droughts in 1.5 and
567 2 °C warmer climates. Hydrol. Earth Syst. Sci. 24, 451-472. doi:10.5194/hess-24-451-2020.

568 Gudmundsson, L., Seneviratne, S.I., 2016. Anthropogenic climate change affects meteorological
569 drought risk in Europe. *Environ. Res. Lett.* 11, 044005. doi:10.1088/1748-
570 9326/11/4/044005.

571 Guerreiro, S.B., Birkinshaw, S., Kilsby, C., Fowler, H.J., Lewis, E., 2017. Dry getting drier – The
572 future of transnational river basins in Iberia. *J. Hydrol. Reg. Studies* 12, 238-252.
573 doi:10.1016/j.ejrh.2017.05.009.

574 Haylock, M.R., Hofstra, N., Klein Tank, A.M.G., Klok, E.J., Jones, P.D., New, M., 2008. A
575 European daily high-resolution gridded data set of surface temperature and precipitation for
576 1950–2006. *J. Geoph. Res.* 113, D20119. doi:10.1029/2008JD010201.

577 Heinrich, G., Gobiet, A., 2012. The future of dry and wet spells in Europe: a comprehensive study
578 based on the ENSEMBLES regional climate models. *Int. J. Climatol.* 32(13), 1951-1970.
579 doi:10.1002/joc.2421.

580 Hellwig, J., Stahl, K., 2018. An assessment of trends and potential future changes in groundwater-
581 baseflow drought based on catchment response times. *Hydrol. Earth Syst. Sci.* 22(12), 6209-
582 6224. doi:10.5194/hess-22-6209-2018.

583 Hirpa, F.A., Salamon, P., Beck, H.E., Lorini, V., Alfieri, L., Zsoter, E., Dadson, S.J., 2018.
584 Calibration of the Global Flood Awareness System (GloFAS) using daily streamflow data. *J.*
585 *Hydrol.* 566, 595-606. doi: 10.1016/j.jhydrol.2018.09.052.

586 Jacob, D., Petersen, J., Eggert, B., Alias, A., Christensen, O.B., Bouwer, L.M., Braun, A., Colette,
587 A., Déqué, M., Georgievski, G., Georgopoulou, E., Gobiet, A., Menut, L., Nikukin, G.,
588 Haensler, A., Hempelmann, N., Jones, C., Keuler, K., Kovats, S., Kröner, N., Kotlarski, S.,
589 Kriegsmann, A., Martin, E., Van Meijgaard, E., Moseley, C., Pfeifer, S., Preuschmann, S.,
590 Radermacher, C., Radtke, K., Rechid, D., Rounsevell, M., Samuelsson, P., Somot, S.,
591 Soussana, J.-F., Teichmann, C., Valentini, R., Vautard, R., Weber, B., Yiou, P., 2014. EURO-

592 CORDEX: New high-resolution climate change projections for European impact research.
593 Reg. Environ Change 14(2), 563-578. doi:10.1007/s10113-013-0499-2.

594 Jacob, D., Kotova, L., Teichmann, C., Sobolowski, S.P., Vautard, R., Donnelly, C., Koutroulis,
595 A.G., Grillakis, M.G., Tsanis, I.K., Damm, A., Sakalli, A., Van Vliet, M.T.H., 2018. Climate
596 Impacts in Europe Under +1.5°C Global Warming. *Earth's Future* 6, 264-285.
597 doi:10.1002/2017EF000710.

598 Jacobs-Crisioni, C., Diogo, V., Perpiña Castillo, C., Baranzelli, C., Batista e Silva, F., Rosina, K.,
599 Kavalov, B., Lavallo, C., 2017. The LUISA Territorial Reference Scenario 2017: A technical
600 description. JRC Technical Reports, EUR 28800 EN, Publications Office of the European
601 Union, Luxembourg, 46 pp. doi:10.2760/902121.

602 Jakubowski, W., Radczuk, L., 2004. Estimation of hydrological drought characteristics
603 NIZOWKA2003 – Software Manual. In: L.M. Tallaksen and H.A.J. van Lanen, eds.
604 Hydrological Drought – Processes and estimation methods for Streamflow and groundwater.
605 Amsterdam: Elsevier Sciences B.V. [CD-ROM].

606 Keramidas, K., Kitous, A., Després, J., Schmitz, A., 2017. POLES-JRC model documentation. EUR
607 28728 EN, Publications Office of the European Union, Luxembourg. ISBN 978-92-79-71801-
608 4. doi:10.2760/225347, JRC107387.

609 Kotlarski, S., Keuler, K., Christensen, O. B., Colette, A., Déqué, M., Gobiet, A., Wulfmeyer, V.,
610 2014. Regional climate modeling on European scales: A joint standard evaluation of the
611 EURO - CORDEX RCM ensemble. *Geosci. Model Develop.* 7(4), 1297-1333.
612 doi:10.5194/gmd-7-1297-2014.

613 Kovats, R., Valentini, R., Bouwer, L., Georgopoulou, E., Jacob, D., Martin, E., Rounsevell, M.,
614 Soussana, J.-F., 2014. Europe, In: *ClimateChange 2014: Impacts, Adaptation, and*
615 *Vulnerability. Part B: Regional Aspects. Contribution of Working Group II to the Fifth*

616 Assessment Report of the Intergovernmental Panel on Climate Change, Eds: Barros, V.R.,
617 C.B. Field, D.J. Dokken, M.D. Mastrandrea, K.J. Mach, T.E. Bilir, M. Chatterjee, K.L. Ebi,
618 Y.O. Estrada, R.C. Genova, B. Girma, E.S. Kissel, A.N. Levy, S. MacCracken, P.R.
619 Mastrandrea, L.L. White, pp. 1267–1326.

620 Lehner, B., Döll, P., Alcamo, J., Henrichs, T., Kaspar, F., 2006. Estimating the impact of global
621 change on flood and drought risks in Europe: a continental integrated analysis. *Clim.*
622 *Change* 75, 273-299. doi:10.1007/s10584-006-6338-4.

623 Marx, A., Kumar, R., Thober, S., Rakovec, O., Wanders, N., Zink, M., Wood, E.F., Pan, M.,
624 Sheffield, J., Samaniego, L., 2018. Climate change alters low flows in Europe under global
625 warming of 1.5, 2, and 3 °C. *Hydrol. Earth Syst. Sci.* 22, 1017-1032. doi:10.5194/hess-22-
626 1017-2018.

627 Mentaschi, L., Alfieri, L., Dottori, F., Cammalleri, C., Bisselink, B., De Roo, A., Feyen, L., 2020.
628 Independence of future changes of river runoff in Europe from the pathway to global
629 warming. *Climate*, 8, 22. doi:10.3390/cli8020022.

630 Metzger, M.J., Bunce, R.G.H., Jongman, R.H.G., Múcher, C.A., Watkins, J.W., 2005. A climatic
631 stratification of the environment of Europe. *Glob. Ecol. Biogeogr.* 14, 549–563.
632 doi:10.1111/j.1466-822X.2005.00190.x.

633 Meyer, V., Becker, N., Markantonis, V., Schwarze, R., van der Bergh, J.C.J.M., Bouwer, L.M.,
634 Bubeck, P., Ciavola, P., Genovese, E., Green, C., Hallagatte, S., Kreibich, H., Lequex, Q.,
635 Logar, I., Papyrakis, E., Pfuertscheller, C., Poussin, J., Przyluski, V., Thielen, A.H.,
636 Viavattene, C., 2013. Assessing the costs of natural hazards – state of the art and knowledge
637 gaps. *Nat. Hazard Earth Syst. Sci.* 13(5), 1351-1373. doi:10.5194/nhess-13-1351-2013.

638 Moss, R.H. et al., 2010. The next generation of scenarios for climate change research and
639 assessment. *Nature* 463(7282), 747-756. doi:10.1038/nature08823.

640 Mubareka, S., Maes, J., Lavalle, C., De Roo, A., 2013. Estimation of water requirements by
641 livestock in Europe. *Ecosyst. Serv.* 4, 139-145. doi:10.1016/j.ecoser.2013.03.001.

642 Naumann, G., Spinoni, J., Vogt, J.V., Barbosa, P., 2015. Assessment of drought damages and their
643 uncertainties in Europe. *Environ. Res. Letters* 10(12). doi:10.1088/1748-
644 9326/10/12/124013.

645 Nerantzaki, S. D., Efstathiou, D., Giannakis, G.V., Kritsotakis, M., Grillakis, M.G., Koutroulis, A.
646 G., Tsanis, I.K., Nikolaidis, N.P., 2019. Climate change impact on the hydrological budget
647 of a large Mediterranean island. *Hydrol. Sci. J.* 64(10), 1190-1203.
648 doi:10.1080/02626667.2019.1630741.

649 Roudier, P., Andersson, J.C.M., Donnelly, C., Feyen, L., Greuell, W., Ludwig, F., 2016. Projections
650 of future floods and hydrological droughts in Europe under a +2°C global warming.
651 *Climatic Change* 135(2), 341-355. doi:10.1007/s10584-015-1570-4.

652 Rudd, A.C., Kay, A.L., Bell, V.A., 2019. National-scale analysis of future river flow and soil
653 moisture droughts: Potential changes in drought characteristics. *Clim. Change* 156(3), 323-
654 340. doi:10.1007/s10584-019-02528-0.

655 Samaniego, L., Thober, S., Kumar, R., Wanders, N., Rakovec, O., Pan, M., Zink, M., Sheffield, J.,
656 Wood, E.F., Marx, A., 2018. Anthropogenic warming exacerbates European soil moisture
657 droughts. *Nat. Clim. Change* 8, 421-426. doi:10.1038/s41558-018-0138-5.

658 Serinaldi, F., 2015. Dismissing return periods! *Stoch. Environ. Res. Risk Assess.* 29, 1179-1189.
659 doi:10.1007/s00477-014-0916-1.

660 Spinoni, J., Vogt, J.V., Naumann, G., Barbosa, P., Dosio, A., 2018. Will drought events become
661 more frequent and severe in Europe? *Int. J. Climatol.* 38(4), 1718-1736.
662 doi:10.1002/joc.5291.

663 Stagge, J.H., Kingston, D.G., Tallaksen, L.M., Hannah, D.M., 2017. Observed drought indices
664 show increasing divergence across Europe. *Sci. Rep.* 7, 14045. doi:10.1038/s41598-017-
665 14283-2.

666 Stagl J., Mayr E., Koch H., Hattermann F.F., Huang S., 2014. Effects of climate change on the
667 hydrological cycle in Central and Eastern Europe. In: Rannow S. and Neubert M. (eds.)
668 Managing Protected Areas in Central and Eastern Europe Under Climate Change. *Advances*
669 *in Global Change Research* 58. Springer, Dordrecht.

670 Stagl J., Hattermann F.F., 2014. Impacts of climate change on the hydrological regime of the
671 Danube river and its tributaries using an ensemble of climate scenarios. *Water* 7(11), 6139-
672 6172, doi:10.3390/w7116139.

673 Stahl, K., Tallaksen, L. M., Hannaford, J., and van Lanen, H. A. J., 2012. Filling the white space on
674 maps of European runoff trends: estimates from a multi-model ensemble. *Hydrol. Earth*
675 *Syst. Sci.* 16, 2035-2047. doi:10.5194/hess-16-2035-2012.

676 Tallaksen, L.M., Van Lanen, H.A.J., 2004. Drought as natural hazard: Introduction. In: L.M.
677 Tallaksen and H.A.J. Van Lanen, (eds.) *Hydrological Drought - Processes and estimation*
678 *methods for streamflow and groundwater*. Amsterdam: Elsevier Sciences B.V., 3-17.

679 Tebaldi C., Arblaster J.M., Knutti, R., 2011. Mapping model agreement on future climate
680 projections. *Geophys Res. Lett.* 38, L23701. doi:10.1029/2011G L0498 63.

681 Teuling, A.J., Van Loon, A.F., Seneviratne, S.I., Lehner, I., Aubinet, M., Heinesch, B., Bernhofer,
682 C., Grünwald, T., Prasse, H., Spank, U., 2013. Evapotranspiration amplifies European
683 summer drought. *Geophys. Res. Letters* 40(10), 2071-2075. doi:10.1002/grl.50495.

684 UNFCCC, 2015. The Paris Agreement. United Nations Framework Convention on Climate Change.
685 Available at: [https://unfccc.int/process-and-meetings/the-paris-agreement/the-paris-](https://unfccc.int/process-and-meetings/the-paris-agreement/the-paris-agreement)
686 [agreement](https://unfccc.int/process-and-meetings/the-paris-agreement/the-paris-agreement).

687 Vandecasteele, I., Bianchi, A., Batista e Silva, F., Lavalle, C., Batelaan, O., 2014. Mapping current
688 and future European public water withdrawals and consumption. *Hydrol. Earth Syst. Sci.* 18,
689 407-416. doi:10.5194/hess-18-407-2014.

690 Van Loon, A.F., Van Lanen, H.A.J., 2012. A process-based typology of hydrological drought.
691 *Hydrol. Earth Syst. Sci.* 16, 1915-1946. doi:10.5194/hess-16-1915-2012.

692 Van Loon, A.F., Van Lanen, H.A.J., 2013. Making the distinction between water scarcity and
693 drought using an observation - modeling framework. *Water Resour. Res.* 49, 1483-1502,
694 doi:10.1002/wrcr.20147.

695 Van Loon, A., Gleeson, T., Clark, J., Van Dijk, A.I.J.M., Stahl, K., Hannaford, J., Di Baldassarre,
696 G., Teuling, A.J., Tallaksen, L.M., Uijlenhoet, R., Hannah, D.M., Sheffield, J., Svoboda, M.,
697 Verdeiren, B., Wagener, T., Rangecroft, S., Wanders, N., Van Lanen, H.A.J., 2016. Drought
698 in the Anthropocene. *Nat. Geosci.* 9, 89-91. doi:10.1038/ngeo2646.

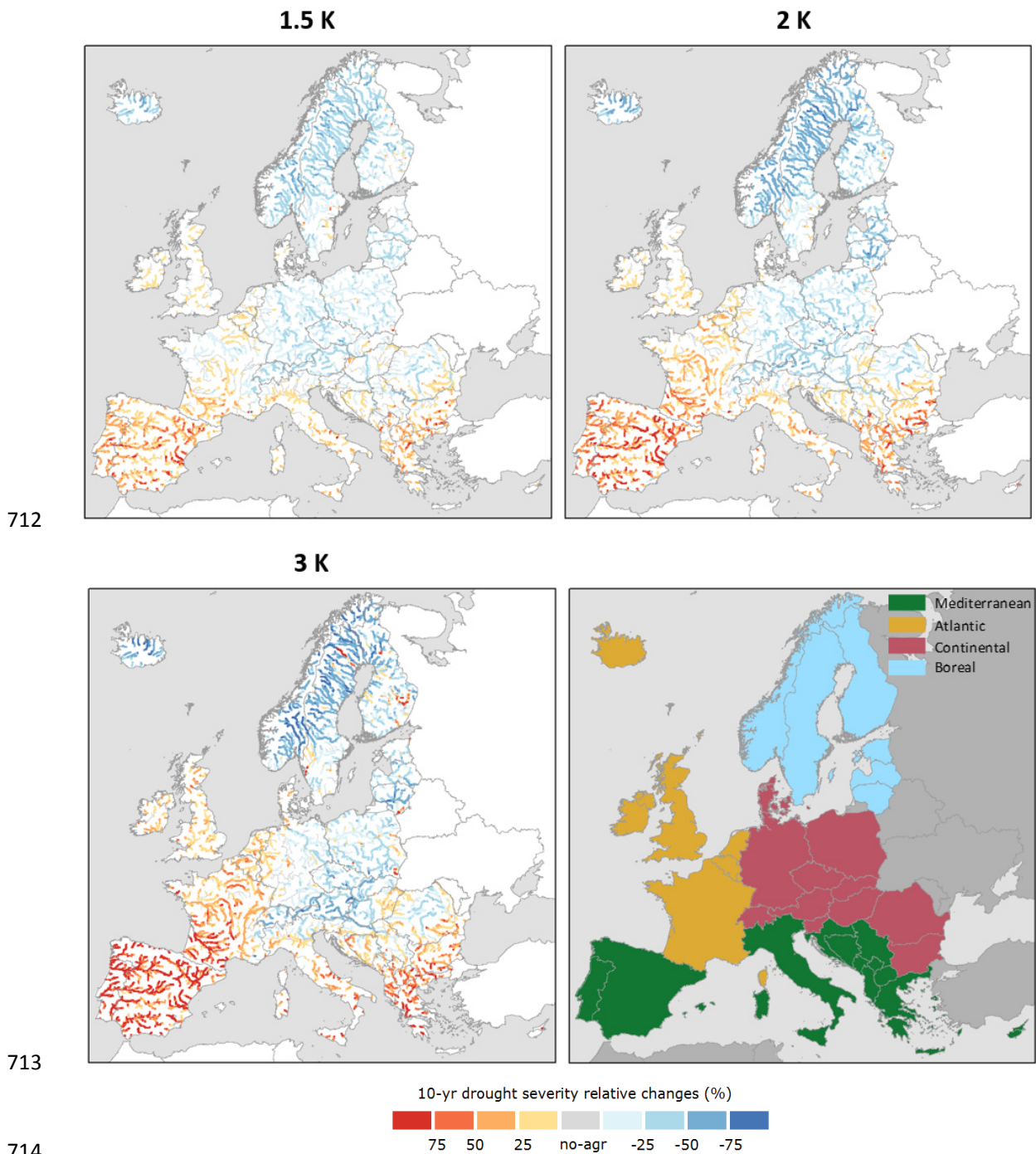
699 Van Tiel, M., Teuling, A.J., Wanders, N., Vis, M.J.P., Stahl, K., Van Loon, A.F., 2018. The role of
700 glacier changes and threshold definition in the characterisation of future streamflow
701 droughts in glacierised catchments. *Hydrol. Earth Syst. Sci.* 22(1), 463-485.
702 doi:10.5194/hess-22-463-2018.

703 Vautard, R., Gobiet, A., Sobolowski, S., Kjellström, E., Stegehuis, A., Watkiss, P., Mendlik, T.,
704 Landgren, O., Nikulin, G., Teichmann, C., Jacob, D., 2014. The European climate under a
705 2 °C global warming. *Environ. Res. Lett.* 9, 034006. doi:10.1088/1748-9326/9/3/034006.

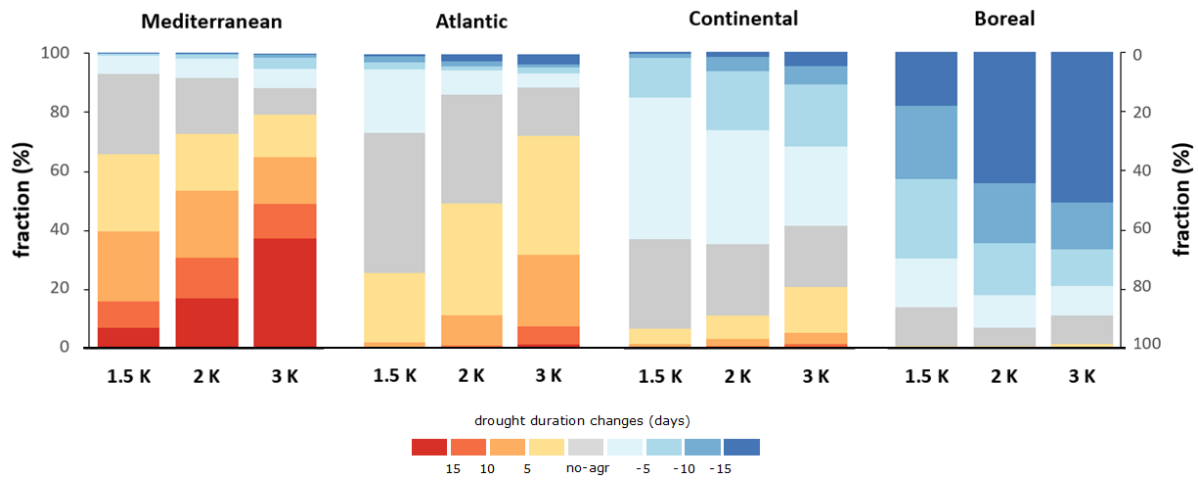
706 Wilhite, D.A., 2000. Drought as a natural hazard: concepts and definitions. In: Wilhite D.A., (eds.)
707 *Droughts: Global Assessment*. London: Routledge, 3-18.

708 Yevjevich, V., 1967. An objective approach to definitions and investigations of continental
709 hydrological droughts. Colorado State University, Fort Collins, Hydrology Paper 23.

710 Zelenhasić, E., Salvai, A., 1987. A method of streamflow drought analysis. *Water Resour. Res.*,
711 23(1), 156-168. doi:10.1029/WR023i001p00156.

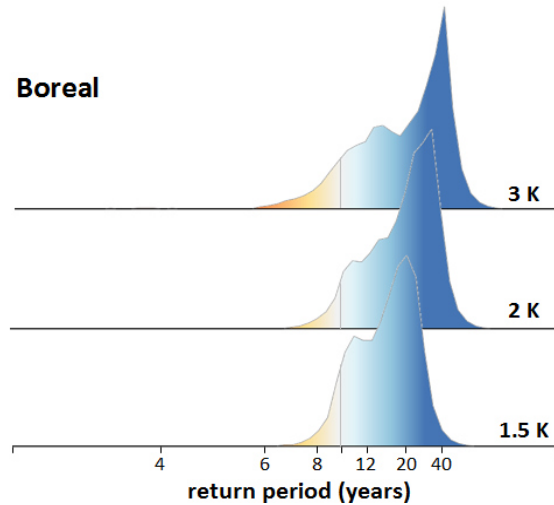
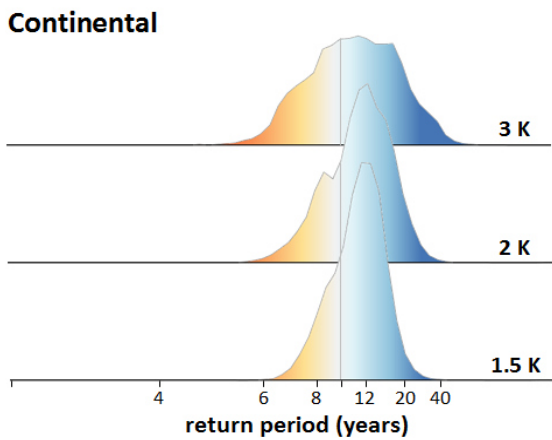
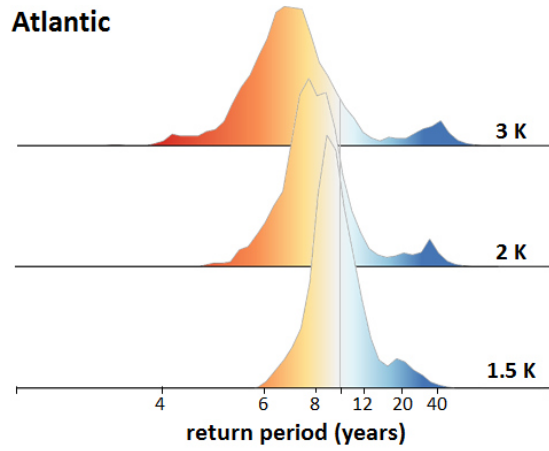
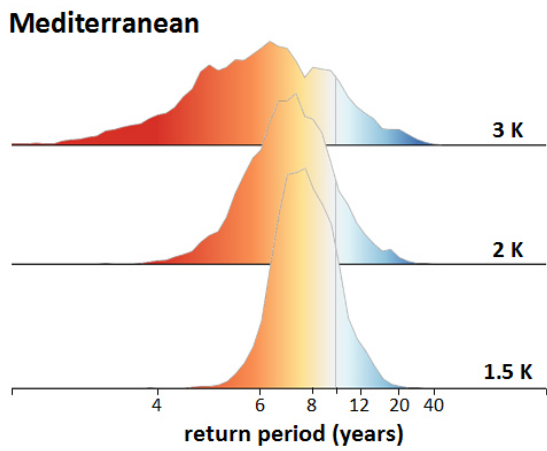


715 **Fig. 1.** Spatial distribution of the ensemble-median relative changes in drought severity of a 10-year
 716 drought (%) between reference period and the three GWLs (1.5 K in the upper-left panel, 2 K in the
 717 upper-right panel, 3 K in the lower-left panel). Positive values represent an increase in drought
 718 severity with warming. The no-agreement (no-agr) class identifies the cells where less than 2/3 of
 719 the climate ensemble members agree on the sign of the change. The lower-right panel represents the
 720 four sub-regions used for aggregation, which are in line with the IPCC AR5 European macro
 721 regions (Kovats et al., 2014).



722

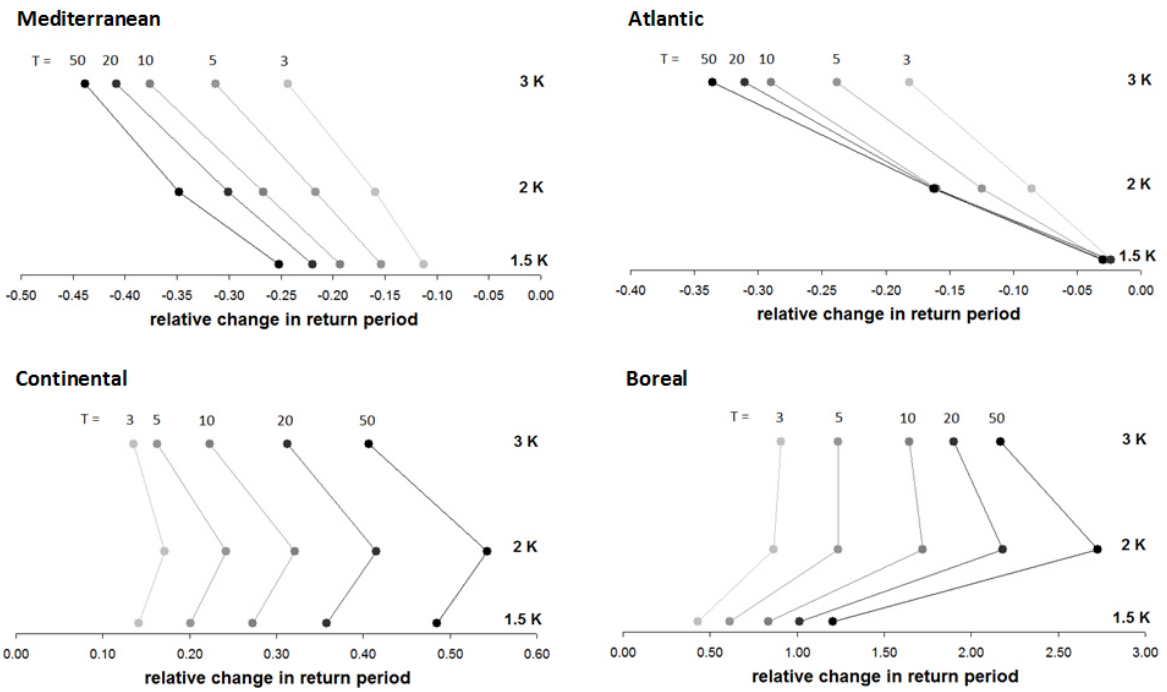
723 **Fig. 2.** Fraction of each sub-region within ranges of change in drought duration (days) for different
 724 GWLs.



725

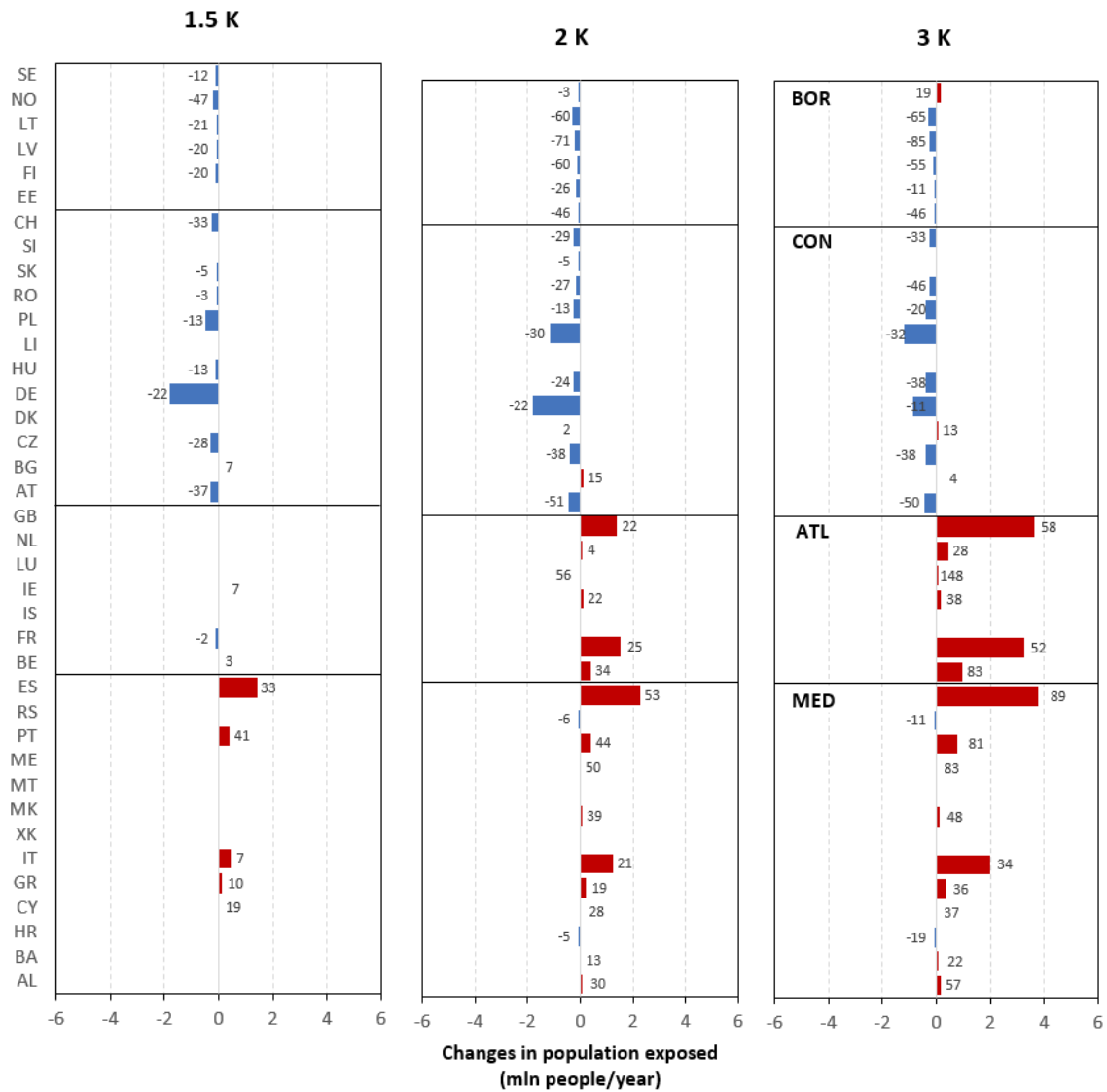
726

727 **Fig. 3.** Frequency distribution of the return period (years) for different GWLs corresponding to an
 728 event with a return period of 10 years in the reference baseline. Values lower (higher) than 10
 729 represent an increase (reduction) in drought frequency. The vertical grey lines demark the 10-year
 730 return period, and the tick marks are uniformly spaced in frequency.



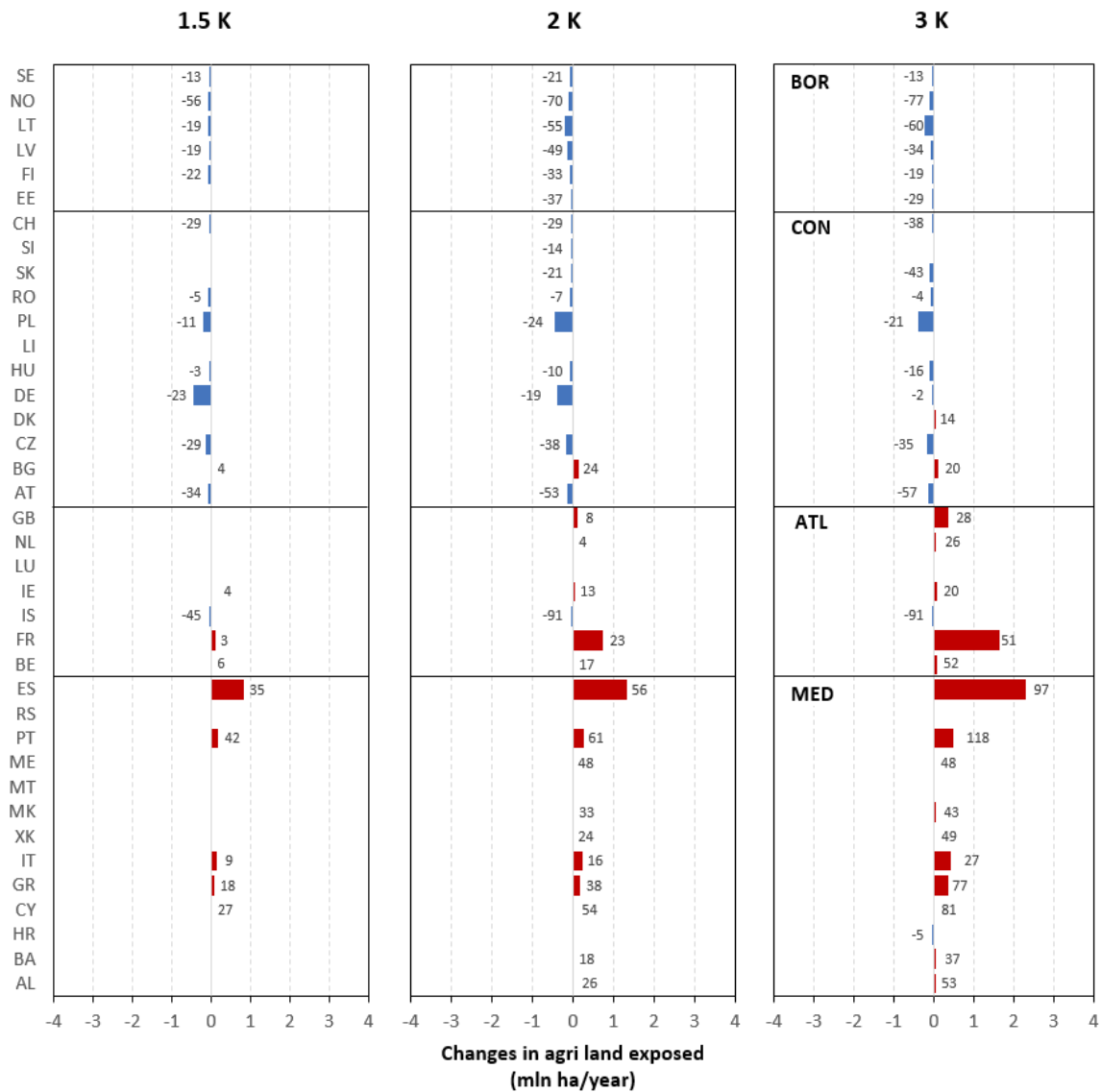
731

732 **Fig. 4.** Relative changes in sub-regional median return period (years) for different GWLs
 733 corresponding to events with a return period of 3, 5, 10, 20 and 50 years in the reference baseline.
 734 Negative (positive) values represent an increase (reduction) in drought frequency.



735

736 **Fig. 5.** Changes in population exposed per country (million people/year). Positive values indicate an
 737 increase in the population exposed. The numbers near the bars represent the percentage changes
 738 relative to the baseline (only if greater than 1%).



739

740 **Fig. 6.** Changes in agricultural land exposed per country (million ha/year). Positive values indicate
 741 an increase in the area exposed. The numbers near the bars represent the percentage changes
 742 relative to the baseline (only if greater than 1%).

743 **Table 1.** Total population exposed per sub-regions (million people/year).

Name	baseline	1.5 K	2 K	3 K
MEDITERRANEAN	14.4	16.8	18.8	21.7
ATLANTIC	16.0	16.1	19.5	24.5
CONTINENTAL	19.6	16.2	15.0	15.5
BOREAL	2.5	2.0	1.7	1.9
TOT	52.5	51.1	55.0	63.6

744

745 **Table 2.** Total agricultural land exposed per sub-regions (million ha/year).

Name	baseline	1.5 K	2 K	3 K
MEDITERRANEAN	5.8	7.1	8.0	9.6
ATLANTIC	5.4	5.5	6.3	7.6
CONTINENTAL	7.7	6.8	6.5	6.8
BOREAL	1.6	1.3	0.9	1.0
TOT	20.5	20.6	21.7	25.0

746